

EXHIBIT A181

Chapter 2

Asbestos and Fibrous Erionite

Ann G. Wylie

Abstract Very narrow fibrils forming bundles of parallel fibers characterize the asbestiform habit. The width of fibrils varies among asbestos types and among occurrences of the same type. The known asbestiform amphiboles have the composition of anthophyllite, tremolite-actinolite-ferroactinolite (prieskaite), cummingtonite-grunerite (amosite and montasite), magnesioarfvedsonite-arfvedsonite, magnesioriebeckite-riebeckite (crocidolite), winchite (Libby amphibole), richterite, and fluoro-edenite-edenite. Amphiboles are common rock-forming minerals that normally occur in a prismatic or massive habit and are not asbestos. The most widely exploited type of asbestos is chrysotile, a member of the serpentine group of minerals. Erionite is a fibrous zeolite; when asbestiform, it is called woolly erionite. This chapter describes the characteristics of these minerals as they occur in an asbestiform habit.

Keywords Asbestos • Tremolite-asbestos • Actinolite-asbestos • Ferroactinolite-asbestos • Anthophyllite-asbestos • Amosite • Crocidolite • Edenite-asbestos • Winchite-asbestos • Richterite-asbestos • Chrysotile-asbestos • Woolly erionite

2.1 Introduction

Asbestos is a naturally occurring, heat-resistant, and chemically inert silicate material that can be readily separated into long, thin, strong fibers with sufficient flexibility to be woven. It may be formed from a number of different minerals that belong to the amphibole or serpentine mineral groups. For thousands of years, the unique properties of asbestos have made it a valuable commodity that has found applications in ceramics, whitewash, paint, fireproof fabrics, reinforced cement, insulation, brake pads, filters, and roofing tiles.

The author has served as a consultant on mineral occurrence, identification, and characterization.

A.G. Wylie (✉)

Laboratory for Mineral Deposits Research, Department of Geology, University of Maryland,
College Park, MD 20742, USA

e-mail: awylie@umd.edu

In the mid-twentieth century, it became clear that the inhalation of asbestos and asbestiform erionite could induce mesothelioma, stimulating extensive research into their physical and chemical characteristics and occurrences in nature. The research focused on relationships between the association of elevated levels of mesothelioma and (1) the size of fibers in the dust cloud, (2) mineral make-up of the fibers, including mineral alterations, intergrowths, and impurities, (3) the biodegradability of the various fibers, (4) surface chemistry, particularly iron content, (5) surface area, and (6) reactivity in vivo. The research has demonstrated that all these characteristics can affect mesotheliomagenicity and that there is considerable variation in carcinogenic potential among asbestiform minerals.

While asbestos and erionite with asbestos-like dimensions are relatively rare, the minerals that form them exist most commonly in a form that is not asbestos. They are common rock-forming minerals and may also be found in soils. Amphiboles and serpentine are found in 6–10% of the land area of the USA and are probably similarly common elsewhere in the world (Wylie and Candela 2015). Erionite is found in geological environments that are common in the western USA and elsewhere; it is only rarely asbestiform (Van Gosen et al. 2013). When disturbed by recreational activities, mining, and excavation for road and building construction, both fragments and fibers of these minerals may become airborne. This chapter will describe the mineralogical characteristics thought to have relevance to biological activity of the major occurrences of commercially exploited amphibole- and serpentine-asbestos, of asbestiform erionite, and of unexploited naturally occurring asbestos and erionite.

2.2 Discussion of Terminology

In modern usage, *asbestos* is applied to a set of minerals from the amphibole and serpentine silicate mineral groups that were mined during the twentieth century and sold as asbestos. The term is also used for asbestiform amphibole that has not been exploited commercially, but is identified as asbestos because of its similarity in habit to commercially exploited asbestos. This would include, for example, the Na-Ca amphiboles that make up the asbestos gangue in the vermiculite deposit at Libby, Montana, some standard reference samples of asbestos, and many museum samples.

The formation of friable mineral fiber is restricted to particular physical and chemical conditions that are limited in their geographical extent. A discussion of geologic occurrences of asbestos in the USA has been provided by Van Gosen (2007). Rock must have been of the appropriate composition and subsequently altered by hot water-rich fluids, dissolving the mineral components until changing conditions resulted in crystallization of secondary minerals in a fibrous form. The *asbestiform habit* describes flexible mineral fibers, formed from parallel or nearly parallel bundles of very thin single crystals, called *fibrils* that are not otherwise regularly aligned. In asbestos, fibrils range in width from about 0.01 to about 0.5 μm . These very small fibrils give a silky luster to asbestos. Fibrils combine to

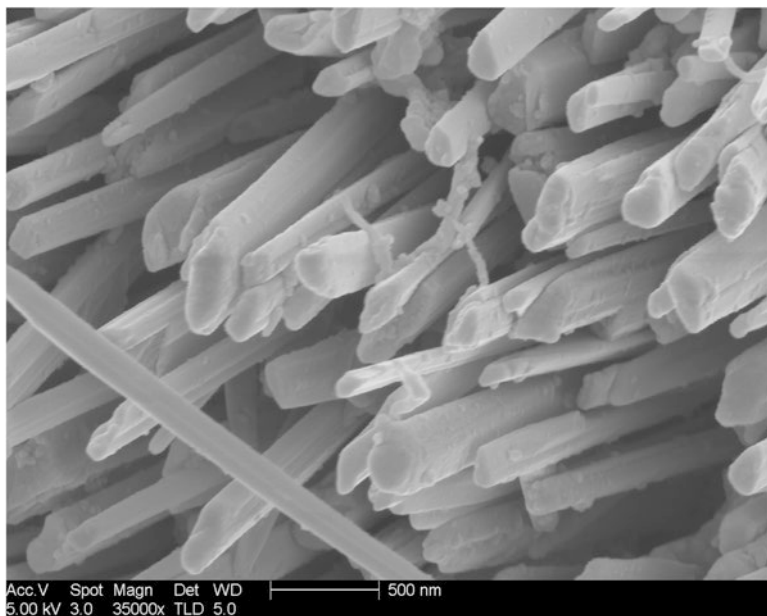


Fig. 2.1 Field emission scanning electron microscopy (FESEM) micrograph of fibril bundle of tremolite-asbestos from North Carolina. Note typical irregularity of the cross section. Photo courtesy R.J. Lee Group

form *fibers* (Fig. 2.1). Asbestos and asbestiform erionite fibers are easily separable with hand pressure, but the ease of *disaggregation* or *separation* into individual fibrils varies among occurrences (Fig. 2.1).

Glassy, brittle fibrils, with width of about 0.5–10 μm or more may accompany asbestos and asbestiform-erionite, or may occur separately. Such glassy brittle fibers of amphibole are referred to as *byssolite* and brittle fibers of serpentine are sometimes referred to as *picrolite* (Fig. 2.2).

In the USA, *regulatory criteria* for counting airborne particles as “fibers” during exposure monitoring are: (1) longer than 5 μm , (2) an aspect ratio of at least 3:1, and (3) visible by optical microscopy. Some portion of a population of airborne asbestos fibers will meet these criteria, but a large portion is below the resolution of the light microscopy ($\approx 0.25 \mu\text{m}$) or is $\leq 5 \mu\text{m}$ in length. A portion of airborne fragmented amphibole, erionite and serpentine particles will also meet these criteria. The National Institute of Occupational Safety and Health has recently clarified that what is being measured are optically visible *Elongated Mineral Particles* (EMP), which are not necessarily fibers in the mineralogical sense (NIOSH 2011). An EMP is, therefore, any particle with a length to width ratio of at least 3:1 whether it is a fiber or fragment; for purposes of occupational exposure monitoring, EMPs must be $>5 \mu\text{m}$.

In this chapter, the term “*fiber*” means an EMP that is a single or twinned crystal bounded by growth surfaces or *crystal faces* (a fibril) or a bundle of such crystals (*fiber bundle*). The term “*fragment*” applies to a particle that is bounded by broken

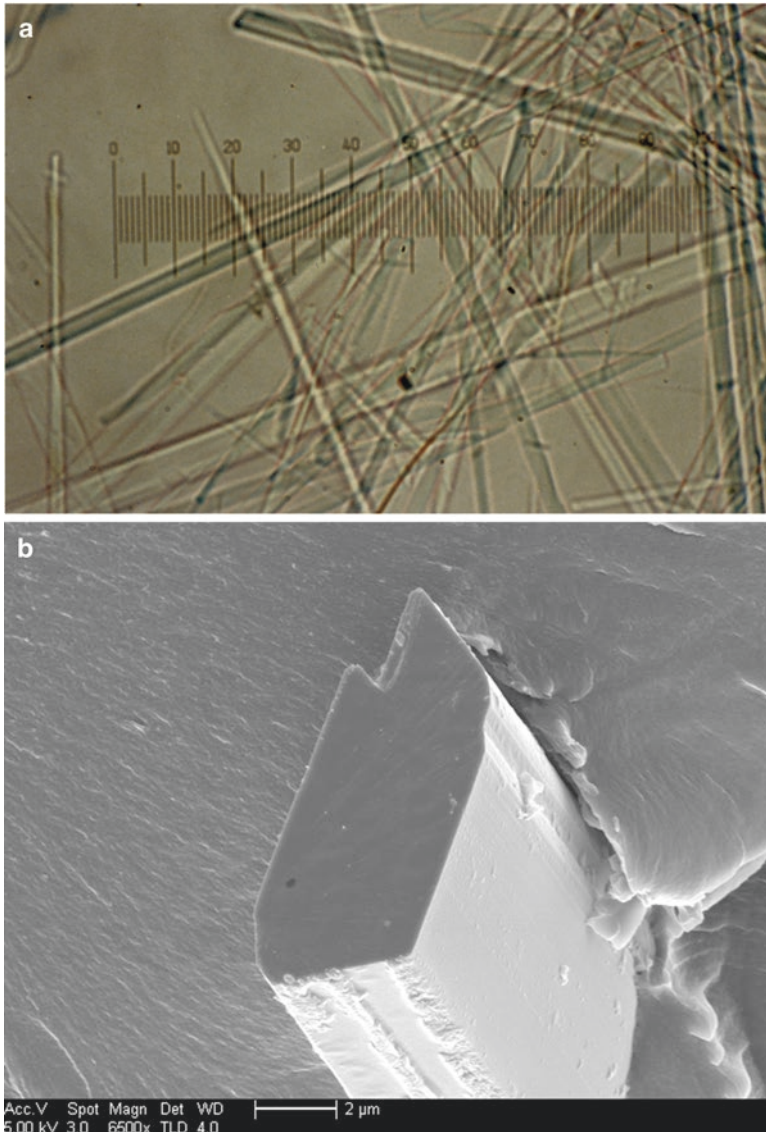


Fig. 2.2 Micrographs of actinolitic byssolite fibers from Austria. **(a)** Photograph of fiber sizes (smallest scale division = 2 μm). **(b)** FESEM micrograph of single fiber (Courtesy R.J. Lee Group). The largest prismatic surfaces that flatten the fiber are {100}

surfaces, originating when rock or brittle fiber is crushed. Fragments may be shaped by geometrically related planes if they possess *cleavage*, defined as the regular way a mineral breaks. Cleavage planes are planes of weakness within the ordered atomic structure of a mineral. In amphiboles, perfect *cleavage* in two directions forms prismatic EMPs, called *cleavage fragments*. Because cleavage arises from weak

structural bonds, the potential for cleavage is the same in every sample of a given mineral. *Parting* resembles cleavage, but the planes of weakness arise from structural defects or inclusions, which are not necessarily present in every sample.

2.3 Amphiboles

There are many *amphibole* minerals, but all are built on double chains of Si_4O_{11} groups linked to each other by a variety of cations. Amphiboles occur in one of two crystal systems: monoclinic and orthorhombic. For both, modern nomenclature is based on the atomic proportions of the major elements assigned to the A, B, C, and T structural sites, following the rules of Leake et al. (1997, 2004) and Hawthorne et al. (2012). The general formula for amphibole is: $\text{AB}_2\text{C}_5\text{T}_8\text{O}_{22}(\text{OH})_2$ where A = \square ,¹ Na, K; B = Na, Ca, Mg, Fe²⁺, Mn²⁺, Li and rarer ions of similar size; C = Mg, Fe²⁺, Mn²⁺, Li, Fe³⁺, Al, Mn³⁺, Cr³⁺, Zr⁴⁺, Ti⁴⁺; T = Si, Al, Ti⁴⁺; and (OH) may be replaced by F, Cl, and O. The A-site is in 10–12-fold coordination, the B- and C-sites are octahedrally coordinated, and the T-site is tetrahedrally coordinated. The structure of amphibole suggests that the A-, B-, and T-sites come in contact with bodily fluids, which would have only limited access to C cations. For this reason, the amphibole formulae in this chapter are written to make the distinctions between A, B, C, and T.

Other systems of nomenclature have been used in the past. The earliest relied primarily on optical properties. Despite changes, there is general agreement among all nomenclature systems used for the last 50 years, although there are notable exceptions, such as the nomenclature of Na-Ca amphiboles, the chemical boundary between tremolite and actinolite, and the nomenclature within the large group of amphiboles generally known as hornblende. Because nomenclature is now strictly tied to crystal system and chemical composition, it may be useful to refer to amphibole-asbestos within solid solutions as, for example, tremolitic-asbestos instead of tremolite-asbestos or actinolitic-asbestos instead of actinolite-asbestos when the exact composition is inferred from qualitative or semi-quantitative chemical analyses or optical properties.

Amphibole minerals and mineral solid solutions known to have formed asbestos are: magnesioriebeckite-riebeckite (crocidolite), cummingtonite-grunerite (amosite and montasite), magnesioarfvedsonite, tremolite-actinolite-ferroactinolite, winchite, richterite, fluoro-edenite-edenite, and anthophyllite. Sometimes, dynamic physical and chemical conditions result in the formation of fibers with several amphibole compositions from the same location. For example, at Libby, MT, and Biancaville, Italy, winchite-asbestos, richterite-asbestos, tremolite-asbestos and edenite-asbestos have been reported (Meeker et al. 2003; Gianfagna et al. 2007). Actinolite-asbestos and crocidolite occur together in South Africa.

Not all amphibole compositions can form asbestos. In particular, Al substitution for Si in the T-site >0.5 atoms per formula unit (apfu) appears to limit the development

¹ \square means the structural site A is empty.

of the asbestiform habit. The highest ^TAl is found in the fluoroedenite-asbestos fibers from Sicily, a region of active volcanism and high heat flow. The generally low ^TAl in asbestos is likely due to the requirement of a temperature for its incorporation into the structure higher than is common in most environments where asbestos forms (Dorling and Zussman 1987).

Amphiboles are well studied, and much is known about their occurrences and the natural variability they show in chemical composition and atomic structure. The optical properties of the common amphiboles are also well known. The reader is referred to major reference works for detailed discussions. These include Hawthorne et al. (2007), Guthrie and Mossman (1993), and Deer et al. (1997).

2.4 Amphibole Fibers and Fragments

Fibers form in open, often fluid-filled spaces or from hydrothermal alteration of pre-existing material in low-pressure environments. Fiber surfaces are often striated from vicinal faces associated with the rapid growth and metastability that arise from rapid precipitation from supersaturated hot water-rich fluids. Prolonged favorable conditions during growth or slow nucleation and crystal growth may result in larger fibril widths. Most fibrils of high quality amphibole asbestos range from 0.03 to $<0.5\ \mu\text{m}$ in width. In some asbestos occurrences, there are several generations of fibril growth, some of which are byssolite fibers of several micrometers in width. Some occurrences of asbestos may be referred to as *mountain leather* or *mountain cork*, when they have been subject to weathering on the earth's surface for long periods of time.

Fibrils are irregular in cross section, only occasionally displaying the expected crystal faces, $\{110\}$, $\{100\}$ and $\{010\}$,² as is evident in Fig. 2.1. However, many analysts report that amphibole fibers encountered in transmission electron microscopy (TEM) and optical studies are frequently flattened near $\{100\}$. A general relationship between width and thickness of fibers of crocidolite and amosite was established by Wylie et al. (1982) from TEM and scanning electron microscopy (SEM) measurements of fibers. It predicts that a fiber $0.1\ \mu\text{m}$ in width would have a thickness of about $0.06\ \mu\text{m}$, while one that is $0.5\ \mu\text{m}$ in width would have a thickness of about $0.2\ \mu\text{m}$.

Amphibole fragments are generally smooth as they are bounded by perfect $\{110\}$ cleavage. They may also be bounded by $\{010\}$ and/or $\{100\}$ parting planes; offsets of faces parallel to cleavage are common (Fig. 2.3).

Structural studies of amphibole asbestos have shown that chain width defects parallel to $\{010\}$ (e.g., a triple chain instead of the double chain characteristic of amphibole), known as Wadsley defects, and twinning or stacking faults parallel to $\{100\}$ are both common. These are particularly well developed in anthophyllite-asbestos but have been reported in all amphibole asbestos and in many samples of common amphibole. Defects may explain the development of large $\{100\}$ surfaces

²Miller Indices, e.g., $\{110\}$, are used to designate the orientation of planes within a crystal structure. A detailed discussion can be found in Bloss (1971) or other mineralogy textbooks.

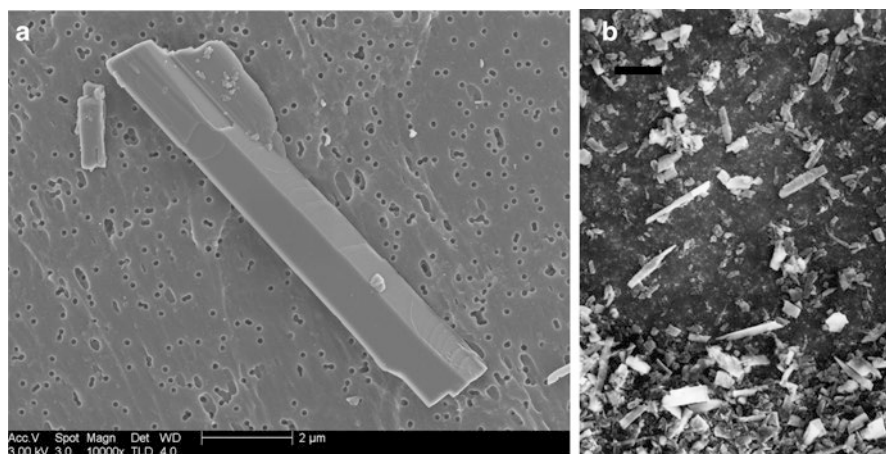


Fig. 2.3 (a) FESEM micrograph of a cleavage fragment of tremolite from Shininess, Scotland (Courtesy R.J. Lee Group). The EMP is formed by perfect $\{110\}$ cleavage. Note offsets on prism surfaces and notched terminus. (b) SEM micrograph of cleavage fragments of grunerite from Homestake Mine, South Dakota (scale bar = 10 μm)

on fibrils. When defects are abundant, parting on $\{100\}$ and $\{010\}$ develops, enhancing the elongation (aspect ratio) of cleavage fragments.

Amphibole surfaces react to some extent with lung fluids, providing varying amounts of Ca, Na, Mg, K, Fe, and Si to the fluid. Some small chemical alterations have been observed on fibers retained in the human lung and there is some evidence for preferential dissolution on $\{100\}$. However, dissolution rates are very slow and fibers persist in the lung many years after exposure. In general, iron and aluminum reduce amphibole solubility in neutral to acidic solutions. Armoring by other minerals, such as talc, might also reduce solubility. In contrast, chrysotile is very soluble in lung fluid (Hume and Rimstidt 1992).

All amphiboles and serpentine would be expected to have tensile strength enhanced by the stable silicon-oxygen chains or sheets that characterize them. However, tensile strength has been shown to increase as the diameter of a fiber decreases (O'Hanley 1986); thus, given its extremely small fibril widths, it is not surprising that the tensile strength of crocidolite from Cape Asbestos Belt in South Africa and from the Hamersley Range in Western Australia has been measured at about 25–48,000 kg/cm^2 (Hodgson 1979) at room temperature; Hodgson (1979) reports tensile strength for amosite as 20–25,000 kg/cm^2 . These compare to the tensile strength of steel piano wire, which is usually given as 25,000 kg/cm^2 . The measured tensile strength of other amphibole-asbestos varies widely, and measurements of tremolitic, actinolitic, and anthophyllite-asbestos, which characteristically have fibrils wider than crocidolite, are usually much lower than that of crocidolite, amosite, and chrysotile. In addition to fibril size, a high frequency of planar defects may also result in an increase in tensile strength.

Surface area of amphibole-asbestos used in manufacturing is quite high, approaching 90,000 cm^2/g as measured by nitrogen absorption, while unprocessed ore may have a surface area an order of magnitude smaller. After ore is mined, it is normally

“fiberized” in the mill to differing degrees, depending on its intended use. Fiberization liberates fibrils, affects fiber size, and increases surface area. In comparing lung fibrosis after exposure to Cape crocidolite, Hamersley crocidolite, amosite, and Paakkila anthophyllite-asbestos, Lippmann and Timbrell (1990) have concluded that it is the surface area of inhaled fibers that controls the degree of lung fibrosis, not mineral type per se, so surface area is an important variable in characterizing asbestos.

The magnetic properties of asbestos have been studied by Timbrell (1975). Amphiboles are paramagnetic and will align in a magnetic field if suspended in air or a liquid. The higher the iron content, in general the lower the field strength required for alignment. Crocidolite, chrysotile, and other fibers generally align with fiber axis parallel to the field. These are referred to as P-fibers. Amosite fibers may be P fibers, but some may align perpendicular to the magnetic field, referred to as N-fibers. Magnetite does not account for the alignment in amphiboles, although it does for some chrysotile. Timbrell reported that a synthetic fluoro-amphibole aligned with its fiber axis transverse at a definite acute angle to the magnetic field (T-fibers), but the relevance to natural mineral fiber is unknown. Variations from P-type fibers might be explained by structural defects such as twinning or by intergrowth of a second mineral phase.

Amphibole fibers and fragments carry a negative charge on their surfaces and a positive charge at their ends. Repulsive forces between fibers, however, are small and settled fibers form an open latticework with many voids. Because surface charge has been shown to be a function of aspect ratio, long narrow fibers will carry a higher charge than shorter or wider ones.

The optical properties of minerals occurring in an asbestiform habit are normally anomalous. Fibrils smaller than about 0.25 μm are not individually resolvable by polarized light microscopy, so it is the properties of a bundle that are observed. In their common form, amphiboles, serpentine, and erionite are birefringent with three principal indices of refraction: *gamma*, *alpha*, and *beta*. Because of the fibrillar habit of asbestos, however, only two indices of refraction can be measured, one parallel and one perpendicular to the fiber axis. Because of this, asbestos is characterized by *parallel extinction* or near parallel extinction. In monoclinic nonasbestiform amphiboles, the vibration directions make an angle with the axis of elongation; they are said to have *oblique extinction*. The anomalous optical properties are described in more detail by Wylie (1979) and by Verkouteren and Wylie (2002).

Generally speaking, each occurrence of amphibole has a distinct chemical composition and has experienced a distinctive geologic history, which determined its habit and the particle sizes it forms when disaggregated (asbestiform habit) and/or fragmented (common mineral forms). Habit and composition of the same mineral can be similar across locations, e.g., crocidolite from Western Australia and the Cape Asbestos Belt of South Africa, but they are more commonly quite different, e.g., crocidolite from other locations differ in both composition and size of fibrils. For occurrences of asbestos of tremolite-actinolite-ferroactinolite composition, the range in properties is quite large. In summary, with few exceptions, generalizations about the nature of asbestos across occurrences and among types without specifying the source location should be made with great care.

2.5 Amphibole-Asbestos

2.5.1 Sodic Amphibole Group

Riebeckite-magnesioriebeckite is a solid solution in the sodic group of amphiboles represented by the end member formula ${}^A\Box{}^B\text{Na}_2{}^C(\text{Mg}, \text{Fe}^{2+})_3{}^C\text{Fe}^{3+}_2{}^T\text{Si}_8\text{O}_{22}(\text{OH})_2$, where the following apfu restrictions apply to substitutions: ${}^T\text{Al} < \text{Fe}^{3+}$, ${}^B\text{Na} > 1.5$, ${}^A(\text{Na} + \text{K}) < 0.50$, $\text{Si} > 7.5$, $\text{Al} < 0.5$, and $(\text{Mn}^{2+} + \text{Mn}^{3+}) < {}^C(\text{Al} + \text{Fe}^{3+} + \text{Fe}^{2+} + \text{Mg})$, $\text{Li} < 0.5$. If ${}^A(\text{Na} + \text{K}) > 0.50$, the amphiboles are called *magnesioarfvedsonite-arfvedsonite*. $\text{Mg}/(\text{Mg} + \text{Fe}^{2+}) = 0.5$ separates *magnesioriebeckite* from *riebeckite* and *magnesioarfvedsonite* from *arfvedsonite*. *Magnesioriebeckite-riebeckite* and *magnesioarfvedsonite-arfvedsonite* are normally blue in color.

The asbestiform variety of *magnesioriebeckite-riebeckite* is known as *crocidolite*, or blue asbestos. Cross fiber veins have been mined in the Hamersley Range, Western Australia, and in the Cape Asbestos Belt, north central South Africa. Cross fiber *crocidolite* has also been mined from the Transvaal Asbestos Belt, northeast South Africa, and from Cochabamba, Bolivia (Redwood, 1993). *Crocidolite* from any locality may be expected to be accompanied by small amounts of magnetite, iron-rich biotite, carbonate, and quartz. In the mines in the Transvaal, kerogen has been reported.

Crocidolite mines in Hamersley Range and Cape Asbestos Belt have provided most of the world's *crocidolite*; in both places, its composition is *riebeckite*. Fibril widths $< 0.1\ \mu\text{m}$ are characteristic as illustrated by Fig. 2.4a and by the frequency distribution of width from the mining and milling aerosol in Fig. 2.4b. The smallest fibrils are on the order of $0.02\ \mu\text{m}$ in width, but rarely $0.5\ \mu\text{m}$ single fibrils occur. The high frequency of airborne fibers of all lengths with widths $< 0.1\ \mu\text{m}$ is unique among the varieties of commercially important amphibole-asbestos (Table 2.1). Cape and Hamersley *crocidolite* disaggregates into component fibrils readily, as reflected by the insensitivity of modal width to length (Table 2.1; Shedd 1985). Frequency distributions derived from bulk samples of long fiber products may be quite different from that of aerosols, reflecting either sampling protocols, removal of the finest fibrils during air processing, or sample preparation protocols, as illustrated in Fig. 2.4c.

Transvaal *crocidolite* fibers are coarser and harsher than Cape fiber. Compositionally, they are *riebeckite* but in some ore, *grunerite* (amosite) asbestos fiber may be intergrown. Cochabamba *crocidolite* fibers are typically light blue, long, and silky. Compositionally, they are *magnesioriebeckite*, but small amounts of another amphibole may be found intergrown. Frequency distributions of the width of *crocidolite* fibers from the Transvaal or from Cochabamba are more likely to resemble those of amosite (Fig. 2.5) than the *crocidolite* depicted in Fig. 2.4. They contain a smaller proportion of fibers less than $0.25\ \mu\text{m}$ and widths extend over a wider range. Modal fiber widths are approximately $0.5\ \mu\text{m}$ and $0.3\ \mu\text{m}$ for Cochabamba, and Transvaal *crocidolite*, respectively (Shedd 1985).

Massive, nonfibrous, common *riebeckite* is found in the rock that encloses *crocidolite* veins in the asbestos mining regions of South Africa, the Hamersley

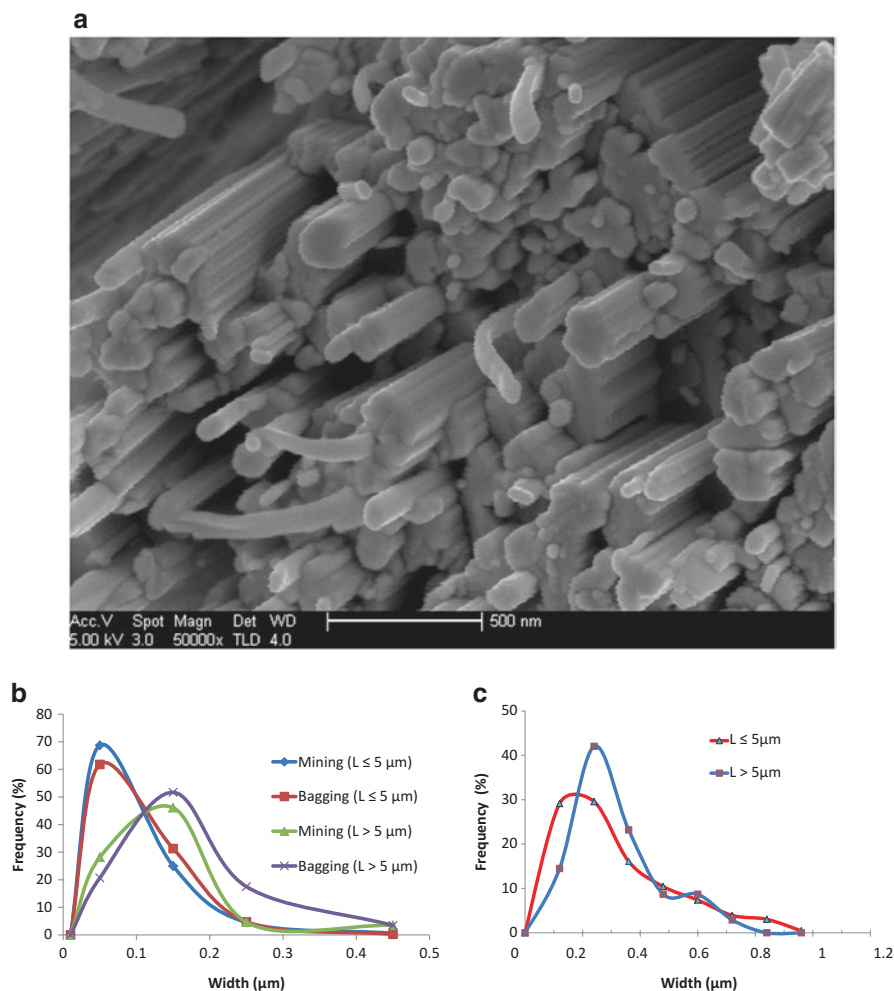


Fig. 2.4 Crocidolite characteristics. **(a)** FESEM micrograph showing fibrillar structure of crocidolite from the Cape asbestos province, South Africa (Courtesy R.J. Lee Group). **(b)** Frequency of width of airborne crocidolite EMPs from the mining and milling environments. Data are taken from Gibbs and Hwang (1980). Magnitude of the largest category of width ($w > 0.3 \mu\text{m}$) is plotted at $0.45 \mu\text{m}$. Lengths range from ≤ 2.5 to $10 \mu\text{m}$: 96% of the fibers from mining and 93% of the fibers from bagging are less than $5 \mu\text{m}$ in length; the modal length for both mining and bagging is $\leq 2.5 \mu\text{m}$. **(c)** Frequency of width of EMPs from bulk crocidolite used as a Standard Reference Material (SRM) by the National Institute of Standards and Technology (NIST). Data are from TEM measurements by Beard et al. (2007); sampling protocol is described by Harper et al. (2008). 23% of fibers measured are $\leq 5 \mu\text{m}$. The range is $2 - 28 \mu\text{m}$, and the modal length is $9.5 \pm 2 \mu\text{m}$. Note that the fibers measured in the bulk material are slightly wider and much longer than those found in the mining and milling aerosol

Range of Australia, and Cochabamba, Bolivia. It is also associated with certain igneous rocks in the western USA and elsewhere. Dimensional characterizations of common riebeckite can be found in Wylie (in press).

Table 2.1 Selected length and width measurements of amphibole-asbestos and amphibole cleavage fragments

	(a) Amosite and crocidolite			(b) Tremolite-ferroactinolite asbestos						Construction ^a
		Airborne amosite ^b	Airborne crocidolite ^c	Asbestos mine ^d	Asbestos mine ^b	raw-NIST SRM	Asbestos mine ^a	raw-NIST SRM		
	Electrical Co.	Shipyard	Mine	Bagging	Tremolite	Tremolite	Tremolite	Prieskaite	Actinolite	
					Korea	India	CA	South Africa	VA	
$L \leq 5 \mu\text{m} >= 1$										
Number measured	90	406			788	125	129	371	91	
Width mode (μm)	0.20 ± 0.05	0.20 ± 0.05	<0.06	0.15 ± 0.05	0.07 ± 0.02	0.22 ± 0.06	0.48 ± 0.06	0.22 ± 0.06	0.72 ± 0.06	
Mean width ± SD (μm)	0.31 ± 0.22	0.31 ± 0.22			0.20 ± 0.19	0.36 ± 0.21	0.68 ± 0.28	0.30 ± 0.15	0.71 ± 0.25	
$5 < L \leq 10 \mu\text{m}$										
Number	121	265			396	30	77	34	32	
Width mode (μm)	0.30 ± 0.05	0.35 ± 0.10	0.15 ± 0.05	0.15 ± 0.05	0.07 ± 0.02	0.33 ± 0.06	1.50 ± 0.24	0.22 ± 0.06	0.66 ± 0.12	
Mean width ± SD (μm)	0.40 ± 0.23	0.41 ± 0.24			0.26 ± 0.33	0.71 ± 0.44	1.48 ± 0.57	0.45 ± 0.20	1.06 ± 0.48	
$10 < L \leq 15 \mu\text{m}$										
Number measured	55	70			136	3	19	9	9	
Width mode (μm)	0.30 ± 0.05	0.20 ± 0.05	0.15 ± 0.05 ^e	0.15 ± 0.05 ^e	0.14 ± 0.05	Undefined	Undefined	Undefined	1.14 ± 0.06	
Mean width ± SD (μm)	0.42 ± 0.29	0.47 ± 0.35			0.39 ± 0.42	1.12 ± 0.64	2.55 ± 0.64	0.45 ± 0.18	1.28 ± 0.52	
	(c) Amphibole-asbestos from Libby Montana				(d) Airborne fragments of common amphibole					
	Airborne	Extracted		Extracted	Stone quarry	Taconite mine	Gold mine	El Dorado Co.		
	town ^f	Mine products ^g		Exfoliation products ^g	VA ^b	Mn ^b	SD ^b	CA ^h		
$L \leq 5 \mu\text{m} >= 1$										
Number measured	1448	245		311	236	58	202	1545		
Width mode (μm)	0.25 ± 0.05	0.16 ± 0.06		0.16 ± 0.06	0.55 ± 0.06	0.55 ± 0.06	0.55 ± 0.06	0.3 ± 0.1		

(continued)

Table 2.1 (continued)

	(a) Amosite and crocidolite			(b) Tremolite-ferroactinolite asbestos						Construction ^a
	Airborne amosite ^b		Airborne crocidolite ^c	Asbestos mine ^d	Asbestos mine ^b	raw-NIST SRM	Asbestos mine ^a	raw-NIST SRM	Asbestos mine ^b	
	Electrical Co.	Shipyards	Mine	Bagging	Tremolite	Tremolite	Tremolite	Tremolite	Prieskaite	Actinolite
					Korea	India	CA	South Africa	VA	
Mean width ± SD (μm)	0.35 ± 0.20	0.28 ± 0.23		0.27 ± 0.19	0.71 ± 0.32	0.70 ± 0.29	0.77 ± 0.29	0.59 ± 0.31		
5 < L ≤ 10 μm										
Number measured	1044	83		151	128	23	126	1080		
Width mode (μm)	0.25 ± 0.05	0.28 ± 0.06		0.28 ± 0.06	1.16 ± 0.06	Undefined	1.10 ± 0.06	0.7 ± 0.1		
Mean width ± SD (μm)	0.59 ± 0.40	0.51 ± 0.33		0.47 ± 0.28	1.48 ± 0.80	1.59 ± 0.44	1.28 ± 0.54	1.29 ± 0.67		
10 < L ≤ 15 μm										
Number measured	429	34		49	40	2	27	367		
Width mode	0.25 ± 0.05	0.27 ± 0.06		0.27 ± 0.06	Undefined	Undefined	Undefined	2.5 ± 0.1		
Mean width ± SD (μm)	0.73 ± 0.56	0.49 ± 0.22		0.54 ± 0.30	2.32 ± 0.93	2.05 ± 1.34	1.91 ± 0.76	2.17 ± 1.14		

Beard et al. (2007)

Wyllie et al. (2015)

Gibb and Hwang (1980)

¹⁴Jenny Verkouteren (personal communication)

The mode is for fibers between 10 and 20 μm in length

EPA (2006)

Atkinson et al. (1981)

^aEcology and the Environment (2005)

2.5.2 Magnesium-Iron-Manganese-Lithium Amphibole Group

2.5.2.1 Cummingtonite-Grunerite

Cummingtonite-grunerite is a solid solution in the magnesium-iron-manganese-lithium group of monoclinic amphiboles represented by the end member formula ${}^A\Box{}^B(\text{Mg}, \text{Fe}^{2+})_2 {}^C(\text{Mg}, \text{Fe}^{2+})_5 {}^T(\text{Si})_8\text{O}_{22}(\text{OH})_2$; the following restrictions to substitutions apply: ${}^B(\text{Ca} + \text{Na}) < 1.0$, ${}^B(\text{Mg}, \text{Fe}, \text{Mn}, \text{Li}) \geq 1.0$, ${}^B\text{Li} < 1.00$, $\text{Si} > 7.0$. $\text{Mg}/(\text{Mg} + \text{Fe}^{2+}) = 0.5$ divides cummingtonite from grunerite. Cummingtonite-grunerite is light to dark brown in color.

The asbestiform variety of cummingtonite-grunerite is known as *amosite* or *brown asbestos*. The silky variety is sometimes called *montasite*. The name amosite

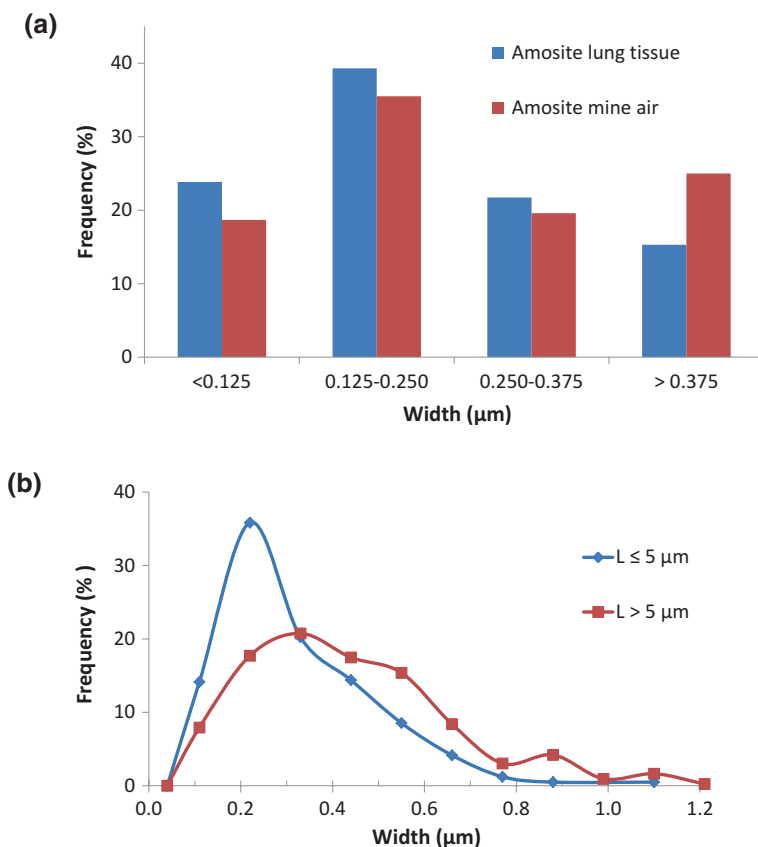


Fig. 2.5 Characteristics of amosite. **(a)** Frequency of width of amosite EMPS from lungs of miners and the mine aerosol, Transvaal, South Africa. Data for fibers of all lengths are taken from TEM measurements of Pooley and Clark (1980). Fibers ranged from <1 to >10 μm in length. Modal length is 2-3 μm, with 8-9% >10 μm and with 32% of airborne and 40% of lung burden fibers longer than 4 μm. **(b)** Frequency of width of amosite EMPS from shipyard aerosol. Fibers range from about 1.5 to >100 μm. Modal length is 2.5 ± 1 μm and about 23% are longer than 5 μm. Particle measurements can be found in Wylie et al. (2015). Many more long fiber bundles are found in the aerosol surrounding the construction of ships than in the mine

is not a proper mineral name; it was derived from the *Asbestos Mines of South Africa* located in the Transvaal Asbestos Belt. These mines have been the only important source of amosite worldwide.

Small amounts of ferroactinolite-asbestos, sometimes referred to as prieskaite, occur in association with amosite in the Transvaal. Magnetite and quartz are common accessory minerals, and minor biotite, pyrite, carbonate, stilpnomelane, kerogen, graphite, and magnesite have been reported in raw asbestos.

Amosite is sometimes described as “harsh.” When the Bureau of Mines was trying to reduce the size of amosite in an air jet mill, the amosite blew a hole through hard-surfaced stainless steel (Campbell et al. 1980). Harshness results when fibrils resist disaggregation, forming larger fibers with less flexibility. Some level of coherence or semi-coherence in the amphibole structure across fibril boundaries has been observed in amosite, and sheet silicates, such as iron-rich talc, serpentine, and chlorite, are normally intergrown with the fibrils; these likely increase amosite’s resistance to disaggregation.

Like crocidolite, frequency distributions of the width of amosite fibrils found in lung tissue and the air of mines and mills normally display a single modal value, as depicted in Fig. 2.5a. Modal widths reported in the literature range from about 0.15 μm for short fibers up to 0.5 μm for fibers longer than 5 μm . Unlike Cape and Hammersley crocidolite, there is a prominent tail on the distribution extending toward larger fiber widths. Such a tail is consistent with fibrils that adhere to one another, resisting disaggregation and resulting in wider fiber bundles, particularly for longer fibers. Of course, amosite may undergo varying degrees of fiberization during processing for different applications, which would be reflected in the size and structure of the tails; some distributions may be multimodal as illustrated in Fig. 2.5b, which shows the frequency of width of amosite fibers in the aerosol of a shipyard. The distribution displays the characteristic increase in the width of longer fibers formed from the bundles of many smaller fibrils.

2.5.2.2 Anthophyllite

Anthophyllite is a solid solution in the Mg-Fe-Mn-Li group of orthorhombic amphiboles represented by the endmember formula ${}^A\Box^B(\text{Mg}, \text{Fe})_2{}^C(\text{Mg}, \text{Fe})_5\text{Si}_8\text{O}_{22}(\text{OH})_2$. Iron-rich anthophyllite is rare. The following restrictions apply to atomic substitutions: ${}^B(\text{Mg}, \text{Fe}^{+2}, \text{Mn}^{+2}, \text{Li}) \geq 1.50$, ${}^B\text{Li} < 0.50$, ${}^T\text{Si} > 7.0$. The largest anthophyllite-asbestos mine is found at Paakkila, Finland. Smaller deposits have been mined in the USA, Sweden, Russia, India, and Pakistan. The risk for mesothelioma from anthophyllite-asbestosis generally is considered to be among the lowest among amphibole-asbestos exposures, and its mineralogical characteristics readily distinguish it from crocidolite and amosite.

Unlike amosite and crocidolite, anthophyllite-asbestos does not normally occur in cross-fiber veins. It is found in pods, masses, and clusters of fibers. Within clusters, parallel fibrils form bundles, but the clusters are not aligned. Its mode of formation results in a less homogeneous material than is characteristic of cross fiber veins.

Talc is always present with anthophyllite-asbestos. It is intergrown in such a way that its structural elements are parallel to those of anthophyllite (the growth is said to be *epitaxial*), and fibers composed only of the mineral talc are commonly associated with anthophyllite-asbestos. Talc is so pervasive that most fiber surfaces are covered

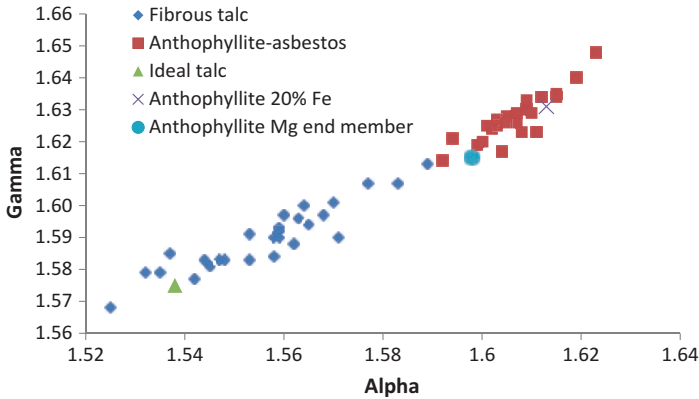


Fig. 2.6 Indices of refraction of fibrous talc, anthophyllite-asbestos, and intergrowths of talc and anthophyllite. Alpha is the smallest principal index of refraction, measured near perpendicular to elongation; gamma is the largest principal index of refraction measured near parallel to elongation. Data for fibrous talc are from Greenwood (1998). Data for anthophyllite-asbestos are from Watson (1999). Indices of refraction vary regularly with water content, $(\text{Mg} + \text{Fe})/\text{SiO}_2$ and Mg/Fe

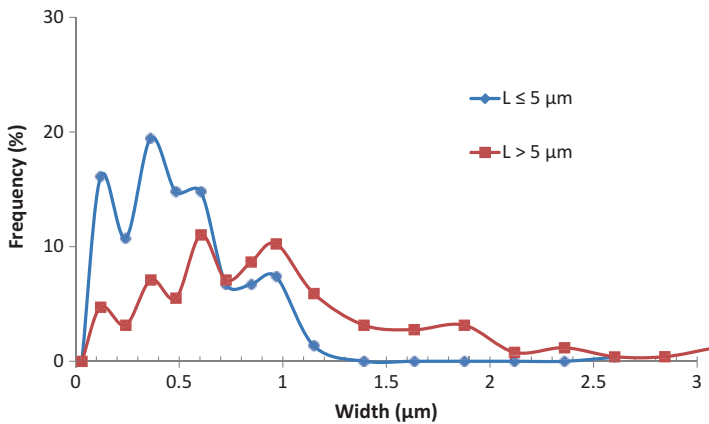


Fig. 2.7 Frequency of width of anthophyllite-asbestos EMPs from Udaipur, India. Data are from TEM measurements by Beard et al. (2007); sampling protocol is described by Harper et al. (2008). About 56% of the fibers measured are $\leq 5 \mu\text{m}$ in length. Lengths ranged from 1 to 40 μm , with a broad mode centered around 4 μm

by it. Some chemical compositions reported for anthophyllite with compositions of $\text{Mg}/(\text{Mg} + \text{Fe})$ between 1.0 and 0.8 may be due primarily to intergrown talc (Watson 1999). Because of similarities in the atomic structure and the close association of these two minerals, a continuum in indices of refraction, birefringence, and chemical composition of fibers exists between end member fibrous talc and anthophyllite-asbestos (Fig. 2.6). Chlorite and serpentine in a variety of forms may also be associated with the anthophyllite-asbestos, and magnetite is a frequent accessory mineral.

A typical width distribution for anthophyllite-asbestos is shown in Fig. 2.7. The distribution shows the presence of very thin fibrils, both long and short, but fibers

with wider widths are very common. Width distributions are frequently multimodal, a characteristic that arises from different generations of fiber growth, or the separation of discrete bundles of fibrils, and/or the incorporation of elongated particles formed by fragmentation. Timbrell et al. (1970) found a multimodal width distribution for anthophyllite-asbestos from Paakkila, Finland, as well. The frequency and size of modal widths will vary among anthophyllite-asbestos occurrences, sampling protocols, and degree of fiberization during processing (Fig. 2.7).

2.5.3 Magnesium-Iron-Manganese-Lithium Amphibole Group

2.5.3.1 Calcic Amphibole Group

Tremolite—Actinolite-Ferroactinolite is a solid solution in the calcic group of monoclinic amphibole represented by the endmember formula: ${}^A\Box{}^B(\text{Ca})_2 {}^C(\text{Mg}, \text{Fe}^{2+})_5 {}^T\text{Si}_8\text{O}_{22}(\text{OH})_2$ with the following restrictions applied to substitutions: ${}^B\text{Ca} \geq 1.50$, ${}^A(\text{Na} + \text{K}) < 0.50$, ${}^A\text{Ca} < 0.50$, and $\text{Si} \geq 7.5$. $\text{Mg}/(\text{Mg} + \text{Fe}^{2+}) > 0.9$ defines the tremolite-actinolite boundary; < 0.5 defines the actinolite-ferroactinolite boundary. Tremolitic amphibole is normally colorless, actinolitic amphibole is green, and ferroactinolitic amphibole is dark green in color. A general discussion of the characteristics of asbestiform and nonasbestiform calcic amphiboles is provided by Dorling and Zussman (1987).

Mesothelioma from exposure to tremolitic-asbestos has been reported from Turkey, Greece, Corsica, New Caledonia, and Cyprus. Tremolite-asbestos is also found associated with chrysotile-asbestos, and it may be incorporated in products containing chrysotile. Small deposits of tremolite- and actinolite-asbestos associated with iron and magnesium-rich rock were mined along the Appalachian Mountains and in the Western USA, particularly in California, during the nineteenth and early twentieth century. Tremolite- and actinolite-asbestos may also be found there in small deposits associated with altered Mg-rich limestone and dolomite. Actinolite-asbestos was used in antiquity in Europe, and asbestos from this series has also been mined in India, Russia, and elsewhere in the world. Tremolite-asbestos makes up a small proportion of the asbestiform amphibole in the vermiculite deposit in Libby, MT (discussed below). Consistent with older terminology, the amphibole-asbestos there was once referred to as tremolite or soda tremolite. Ferroactinolite-asbestos occurs in the Transvaal Asbestos Belt, where it is known as prieskaite.

Because members of this series are among the most common amphiboles, occurrences in the asbestiform habit are widespread although their exploitation as asbestos has been limited. Samples from many locations have been studied, and although asbestiform, they display a wide range in the size of the fibrils that make them up. Width and length data from five members of this series are provided in Table 2.1. Fibrils range from less than 0.1 to as much 0.66 μm . Only the asbestos from Korea has dimensions that are comparable to amosite and crocidolite. Mean widths for tremolite-asbestos that accompanies chrysotile-asbestos from Thetford, Quebec,

have been reported from about 0.21–0.25 μm for fibers less than 5 μm and about 0.3–0.35 μm for longer fibers. This asbestos is likely more similar to Indian tremolite-asbestos in Table 2.1 than to Korean asbestos or the raw-NIST-SRM. The range in habits is also illustrated in Fig. 2.8, which depicts three tremolite-asbestos samples: Korea, the raw-NIST SRM from California, and the asbestos found in the Whitewash at Metsovo, Greece. The dimensions and the macroscopic appearance of the raw-NIST SRM are consistent with wide glassy fibers, so this asbestos appears to have characteristics that grade into byssolite.

Fluoro-edenite. Edenite-ferroedenite is a solid solution in the calcic group of monoclinic amphiboles represented by the end member formula $^A(\text{Na},\text{K})^B(\text{Ca}, \text{Mg}, \text{Fe}^{2+})_2(\text{Mg}, \text{Fe}^{2+}, \text{Mn}, \text{Li})_5^T(\text{Si},\text{Al})_8\text{O}_{22}(\text{OH},\text{F})_2$ with the following restrictions applied to substitutions: $^B\text{Ca} \geq 1.50$, $^A(\text{Na} + \text{K}) \geq 0.50$, $6.5 < \text{Si} < 7.5$, and $\text{Ti} < 0.50$. The addition of the prefix fluoro- means that $F > 1.0$ in substitution for (OH). Mesothelioma from exposure to fluoro-edenite asbestos has been reported from Biancavilla, Sicily, Italy, where it is accompanied by small amounts of winchite-, richterite-, and tremolite-asbestos (Gianfagna et al. 2007). Minor feldspar, pyroxene, apatite, and magnetite are common. The widths of fibers with $L > 5 \mu\text{m}$ from Biancavilla follow a frequency distribution similar to that of Indian tremolite-asbestos 2 shown in Fig. 2.8, with a modal width of 0.2–0.4 for fibers $> 5 \mu\text{m}$ (Paoletti and Bruni 2009).

2.5.3.2 Sodic-Calcic Amphibole Group

The *sodic-calcic amphibole* group contains several monoclinic amphiboles that are known to occur as asbestos including members of the solid solutions *richterite-ferrichterite* represented by the endmember formula $^A\text{Na}^B(\text{CaNa})^C(\text{Mg},\text{Fe})_5^T\text{Si}_8\text{O}_{22}(\text{OH})_2$ and *winchite-ferrowinchite*, represented by the end member formula $^A\Box^B(\text{CaNa})^C(\text{Mg},\text{Fe}^{2+})_4^C(\text{Al},\text{Fe}^{3+})^T\text{Si}_8\text{O}_{22}(\text{OH})_2$. The following restrictions apply to substitutions for richterite-ferrichterite: $^A(\text{Na} + \text{K}) \geq 0.50$, $^B(\text{Ca} + \text{Na}) \geq 1.00$, $0.50 < ^B\text{Na} < 1.50$ and $\text{Si} > 7.5$; for winchite-ferrowinchite: $^A(\text{Na} + \text{K}) < 0.50$, $^B(\text{Ca} + \text{Na}) \geq 1.00$, $0.50 < ^B\text{Na} < 1.50$ and $\text{Si} > 7.5$.

Amphibole-asbestos is abundant as gangue in the vermiculite ore mined at Libby, MT. Studies of its mineralogy have shown that winchite-asbestos is by far the most abundant, followed by richterite-asbestos and tremolite-asbestos; a small amount of edenite-asbestos may also be present (Meeker et al. 2003). The asbestos occurs in unaligned masses and clusters of parallel fibril bundles. The same amphibole-asbestos types are found at Biancavilla, Italy, although at that location edenite-asbestos is the most abundant.

Representative frequency distributions of the width of asbestos fibrils from Libby are shown in Fig. 2.9 and dimensional data are also provided in Table 2.1. Short fibers are dominated by particles that are 0.1–0.2 μm in width with very few wider particles. Long fibers are characterized by modal width of about 0.3 μm , with another distinctive mode at about 0.55 μm .

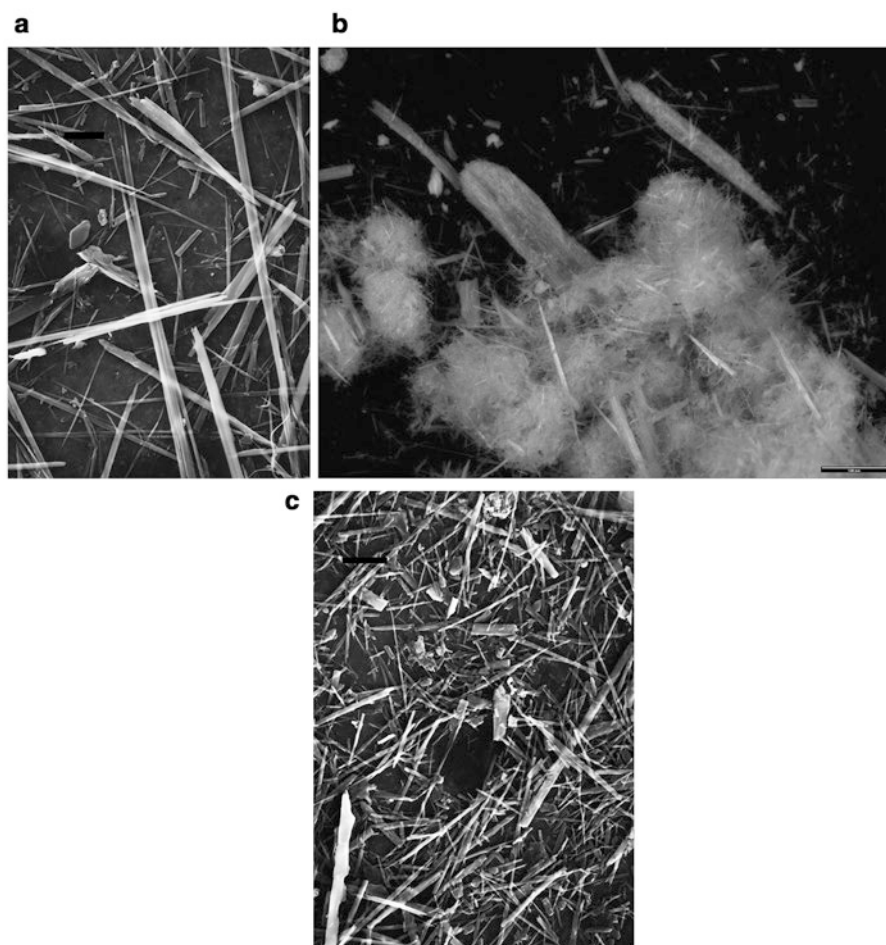


Fig. 2.8 Variability in the habits of asbestiform amphiboles are illustrated by three occurrences of tremolite-asbestos. (a) SEM micrograph of tremolite-asbestos from Korea (scale bar = 5 μm). (b) Macrograph of tremolite-asbestos from Condo Deposit, CA, NIST SRM 1867a (Courtesy R.J. Lee Group). This material contains many glassy fibers, more characteristic of byssolite than asbestos. (c) SEM micrograph of tremolite-asbestos from whitewash used in Metsovo, Greece, where exposure is associated with excess mesothelioma (scale bar = 5 μm)

2.5.4 Dimensional Characteristics of Common Amphibole

Many studies have examined common amphibole in mining aerosols. Others have looked at common amphibole dusts derived from comminution in the laboratory or directly measured in dusty environments. Populations of airborne and bulk cleavage fragments share dimensional characteristics, which are generalized in Fig. 2.10.

The frequencies of width for both long and short cleavage fragments of amphibole are multimodal. The smallest mode is normally $<0.2 \mu\text{m}$, but none of these

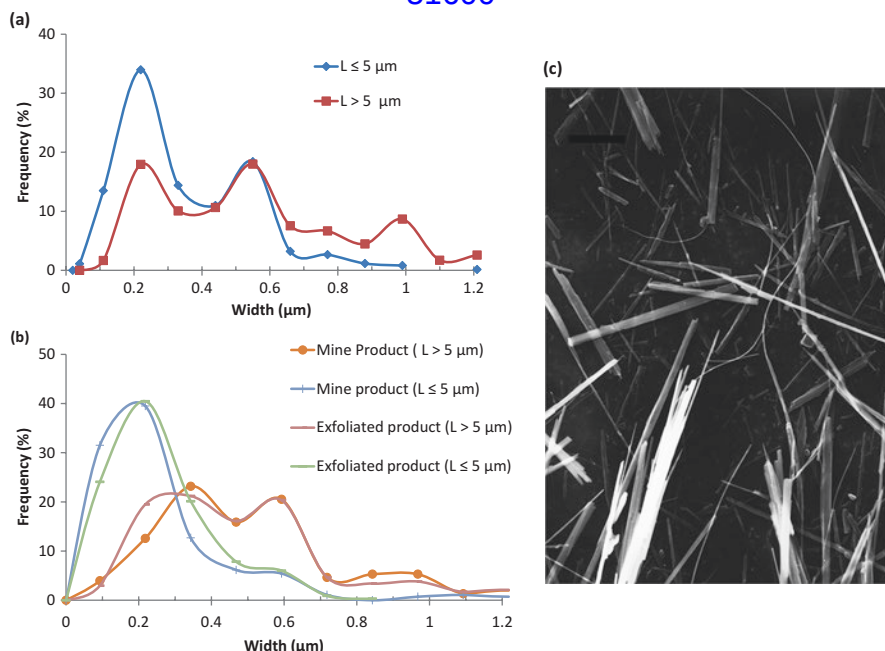


Fig. 2.9 Amphibole-asbestos from Libby, Montana. **(a)** Frequency of width of airborne amphibole asbestos EMPs collected from the town of Libby, MT. Data are from TEM measurements by the Environmental Protection Agency (Data courtesy R.J. Lee). Fibers range from about 1.5 to 95 μm in length, with modal lengths of $3.5 \pm 1 \mu\text{m}$ and $9.5 \pm 2 \mu\text{m}$. **(b)** Frequency of width of amphibole-asbestos EMPs extracted from mined and exfoliated vermiculite, Grace Mine, Libby, MT. Data are from TEM measurements by Atkinson et al. (1981). Fibers ranged from 1 to 80 μm for mine products and <1 to $>50 \mu\text{m}$ in exfoliated materials. Modal length for both populations was about $2.5 \pm 1 \mu\text{m}$. Approximately 64% of fibers from untreated vermiculite and 59% of the fibers extracted from the exfoliated vermiculite were $\leq 5 \mu\text{m}$ in length. **(c)** SEM micrograph of amphibole-asbestos from Libby (scale bar = 10 μm). The bimodal width and length distributions suggest several periods of fiber growth. This is reflected in the micrograph, which shows that wide fibers, narrow fibers and fiber bundles compose the material

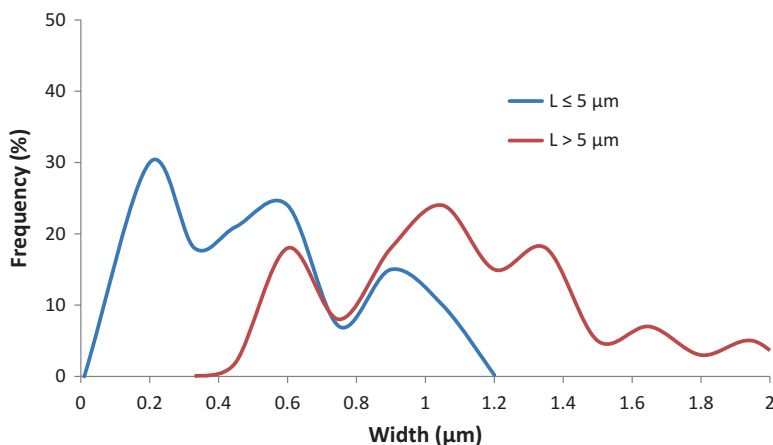


Fig. 2.10 Frequency of width typical of common amphibole cleavage fragment EMPs. Data can be found in Wylie et al. (2015). Between 20 and 50% of the EMPs in most populations are longer than 5 μm . Typical ranges of length are 1–50 μm

narrow particles are longer than 5 μm . Table 2.1 provides data on dimensions of airborne amphibole cleavage fragments. Amphibole particles that are longer than 5 μm are characteristically wider than 0.33 μm , and longer particles are characterized by even larger widths. For any length range, the variance in width can be quite large as indicated by the large standard deviations associate with mean width.

2.6 Serpentine

There are three types of structurally distinct *serpentine minerals*: *antigorite*, *lizardite*, and *chrysotile*. The structure of the serpentine minerals is based on a 1:1 layer motif, comprising tetrahedral $[\text{Si}_2\text{O}_5]$ and octahedral $[\text{Mg}_3\text{O}_2(\text{OH})_4]$ sheets. Variation in stacking sequences of this composite layer results in multiple polytypes. There is a mismatch between the lateral dimensions of the silicate and hydroxide layers, which can be accommodated by curvature of the composite layer, with the octahedral layer on the outside. Two of the serpentine minerals involve curved layers. Antigorite possesses a modulated layered structure that alternates the sense of bending, producing a corrugated sheet. In chrysotile, the composite layers roll up into spiral or helical scrolls, resulting in tubular fibers. The lizardite structure can perhaps accommodate the structural misfit by a small crystallite size, slight curvature, chemical substitutions, and/or structural defects, but a full explanation is lacking. The three minerals have the same nominal, ideal chemical composition $\text{Mg}_3\text{Si}_2\text{O}_5(\text{OH})_4$, although antigorite contains more Mg and hydroxyl and less Si than the ideal composition.

Serpentine minerals occur together. Chrysotile-asbestos is commonly found with lizardite, but all three polymorphs may occur together. In some cases, they are intergrown on the molecular scale. In others, one type dominates. Most serpentine-asbestos is chrysotile, although antigorite-asbestos has been reported from Australia (Keeling et al. 2008). A triple-chain mineral with a chemical composition similar to serpentine, $(\text{Mg}, \text{Fe}^{2+}, \text{Fe}^{3+}, \text{Mn}^{2+})_{42}\text{Si}_{16}\text{O}_{54}(\text{OH})_{40}$, and associated with massive serpentine and chrysotile-asbestos, has been mined as asbestos in Balangero, Italy, which gives the mineral its name, *balangeroite*. Serpentine also exists in splintery veins in a habit referred to as *picrolite*. Picrolite is composed of chrysotile and/or antigorite, but chrysotile fibrils are normally not liberated when the picrolite is fragmented. *Carlosturanite*, a double- and triple-chain silicate is found intergrown with antigorite and/or chrysotile in picrolite.

The most common chemical substitutions are Fe and Ni for Mg (*pecoraite* is the name used for the naturally occurring nickel analogue of chrysotile) and Al and Fe^{+3} for Si. Where found together in nature, the polymorphs may differ in their Al_2O_3 and FeO contents. While small amounts of Al and Fe^{+3} are common, iron-free occurrences of all three polymorphs are known. Chrysotile with $\text{FeO} > 4$ weight % has been reported. For a detailed discussion of the chemistry, structure and occurrences of serpentine, the reader is referred to Deer et al. (2009) and Guthrie and Mossman (1993).

2.6.1 Chrysotile-Asbestos

Chrysotile-asbestos occurs as veins or masses of parallel fibers in massive serpentine. An example is shown in Fig. 2.11a. In veins, chrysotile appears gold to light green, but when it is fiberized, it is almost colorless and may be referred to as *white asbestos*. Most chrysotile-asbestos comes from mines that exploit cross-fiber veins with magnetite, talc, chlorite, anthophyllite and tremolite-asbestos as accessory minerals. However, slip fiber veins have also been exploited such as in the Carey deposit in Quebec, Canada. The abundance of associated tremolite-asbestos varies significantly; Addison and Davies (1990) reported that the tremolite content (both fibers and fragments) of chrysotile-asbestos varies from undetected (<0.01%) to 0.6%. In Canada, it is a minor but ubiquitous component of the asbestos mined at Thetford Mines, but it is less common in the ore bodies at Asbestos, Quebec. Some attribute the higher rate of mesothelioma among miners and millers at Thetford to the tremolite-asbestos alone, and many have proposed that chrysotile-asbestos is not mesotheliomagenic. For a discussion of the health effects of chrysotile-asbestos, the reader is referred to Nolan et al. (2001).

The Coalinga asbestos deposit in California is a mass fiber deposit that did not produce a long fiber product, although fiber bundles as long as 30–40 μm occur. Small cross fiber veins were present but were inconsequential in ore tonnage (Mumpton and Thompson 1975.)

The structural scroll of chrysotile provides an interior tube that is normally hollow, but some fibrils have material filling their cores, which may account for observed variations in density and surface area measurements. These tubes are on the order of 70–80 Å in diameter; the diameter of a typical fibril is 220–270 Å but may range up to 650 Å. Fig. 2.11b shows the frequency distribution of width of a highly disaggregated chrysotile-asbestos from the Coalinga deposit. Fig. 2.11c depicts the frequency distribution of a bulk sample of an air-classified long fiber chrysotile-asbestos from Quebec (Fig. 2.11).

The very small diameter of chrysotile fibers promotes high tensile strength, which approaches that of crocidolite (Hodgson 1979). Like other high tensile strength asbestos, when ground in a mortar and pestle, fibers form matted aggregates and do not readily reduce to a powder.

Chrysotile contains a negligible amount of iron, yet its fibers normally align parallel to magnetic fields, indicating small magnetite particles among the fibers. If the material is well fiberized, it may be possible to use magnetic separation techniques to remove the associated magnetite.

A hexagonal array of hydroxyl groups of $\text{Mg}(\text{OH})_2$ forms the surface of chrysotile. It will likely form at least transient hydrogen bonds to water, so chrysotile is hydrophilic. Lung fluid is normally undersaturated with respect to Mg and Si, and chrysotile will dissolve with time (Hume and Rimstidt 1992). Surface charge is strongly positive and settled dusts can form dense sediments.

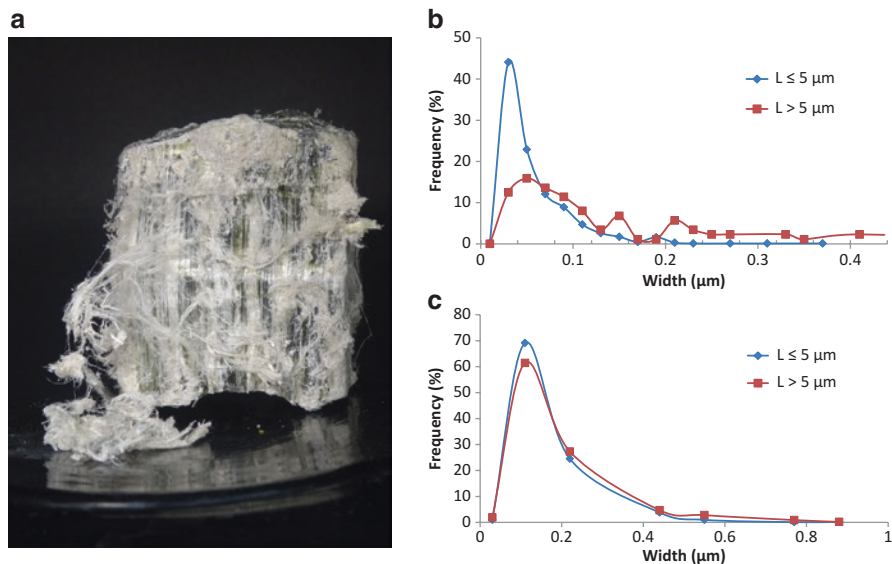


Fig. 2.11 (a) Chrysotile. Cross fiber vein, Quebec, Canada. Frequency distributions of width from two chrysotile populations are shown in (b) and (c). Samples prepared as reference materials for the National Institute of Environmental Health Sciences (NIEHS) (Campbell et al. 1980). Particle measurements can be found in Wylie and Virta (2016). (a) Frequency of width of chrysotile EMPs from Coalinga Deposit, CA, measured by TEM. The range of lengths measured is 0.1–45 μm. The modal length is $\leq 1 \mu\text{m}$, and 92% of the fibers have $L \leq 5 \mu\text{m}$. (b) Frequency of width of a long fiber chrysotile EMPs from a mill product of the Jeffrey Mine, Quebec, Canada, measured by SEM. Lengths range from 0.4 to almost 1000 μm, with a broad mode at about 2 μm. 68% of fibers have $L \leq 5 \mu\text{m}$

2.6.2 Other Serpentine EMPs

Keeling et al. (2008) report that about 18% of the antigorite-asbestos fibers from Australia that are longer than 5 μm are less than 0.25 μm in width, consistent with other forms of commercially available asbestos. Laths as wide as 4 μm are also present.

Picrolite is a splintery habit of serpentine. It occurs in veins and may have formed following thermal metamorphism of cross-fiber chrysotile veins. Under the optical microscopy, picrolite forms splinter lath-shaped EMPs but dimensional data on aerosol-sized particles are lacking.

2.7 The Zeolite Erionite

Erionite is one of a large group of silicate minerals called zeolites, microporous aluminosilicates, commonly found in altered volcanic tuffs, volcanic ash and muds derived from them. Zeolite-bearing volcanic tuff is widely used as a building stone. Many zeolites are used in water treatment, as a soil additive for horticulture and soil remediation, as a catalyst in hydrocarbon cracking, and in solar energy heating, cooling, and storage. For a detailed discussion of the mineralogy of the zeolites, the reader is referred to Deer et al. (2004) and Bish and Ming (2001).

Erionite belongs to a class of zeolites that is built on six-member rings of $[\text{SiO}_4]^{-4}$ tetrahedra in which Al substitutes for Si in a ratio of approximately 1:3. There are three species in the erionite series: erionite-Na, erionite-K, and erionite-Ca. The chemical composition of the series is represented by the formula $\text{K}_2(\text{Na}, \text{K}, \text{Ca}_{0.5})_7\text{Al}_9\text{Si}_{27}\text{O}_{72}\cdot 30\text{H}_2\text{O}$. A compilation of the chemistry of many occurrences of the erionite series can be found in Dogan and Dogan (2008).

Zeolites are known for their ion exchange capacities, and complete replacement of Na by K, Rb, Cs, and Ca in erionite has been attained in the laboratory. Erionite is nominally iron free, but iron may be captured on its surface (Fe^{3+}) or by ion exchange (Fe^{2+}) in vivo (Eborn and Aust 1995). The density of erionite is low for silicate minerals, about 2 gm/cm^3 , which can be attributed to a water content of almost 20 wt.% H_2O , rendering erionite unstable under an electron beam under normal operating conditions and making chemical analysis by EDS problematic.

Erionite frequently occurs with other zeolites, notably clinoptilolite, phillipsite, and chabazite, and may be epitaxially intergrown with the zeolite offretite or overgrown on the zeolite levyne. Iron oxides, iron hydroxides, and iron-rich clay (nontronite) have been reported as nanoparticles on fiber surfaces. Quartz, feldspar, and clay are commonly associated minerals. The detection limit for erionite in altered volcanic rocks by XRD is estimated to be 0.1–0.5% (Bish and Chipera 1991).

Most zeolites are not fibrous, although some form EMPs when crushed, but erionite is notable for a fibrous habit. The zeolite *mordenite* is also commonly fibrous, and ferrierite and phillipsite may sometimes occur as fibers, but none of these occurs in an asbestiform habit.

The type locality for erionite is Durkee Oregon, where it occurs in the asbestiform habit and is known as *woolly erionite* (Fig. 2.12). This material has been well characterized by Cametti et al. (2013). *Woolly erionite* has also been found in Lander County and Churchill County, Nevada (Gude and Sheppard 1981).

Woolly erionite has been shown to be a potent animal carcinogen, and exposure to fibrous erionite found in building stone and white wash in the Cappadocia region of Turkey is associated with a marked excess of mesothelioma. Similar occurrences and disease excess have recently been reported from Mexico and Nevada. Photographs, descriptions, and size and shape characterizations of erionite and other zeolites have been provided by Shedd et al. (1982). Van Gosen et al. (2013) have summarized erionite occurrences in the USA.

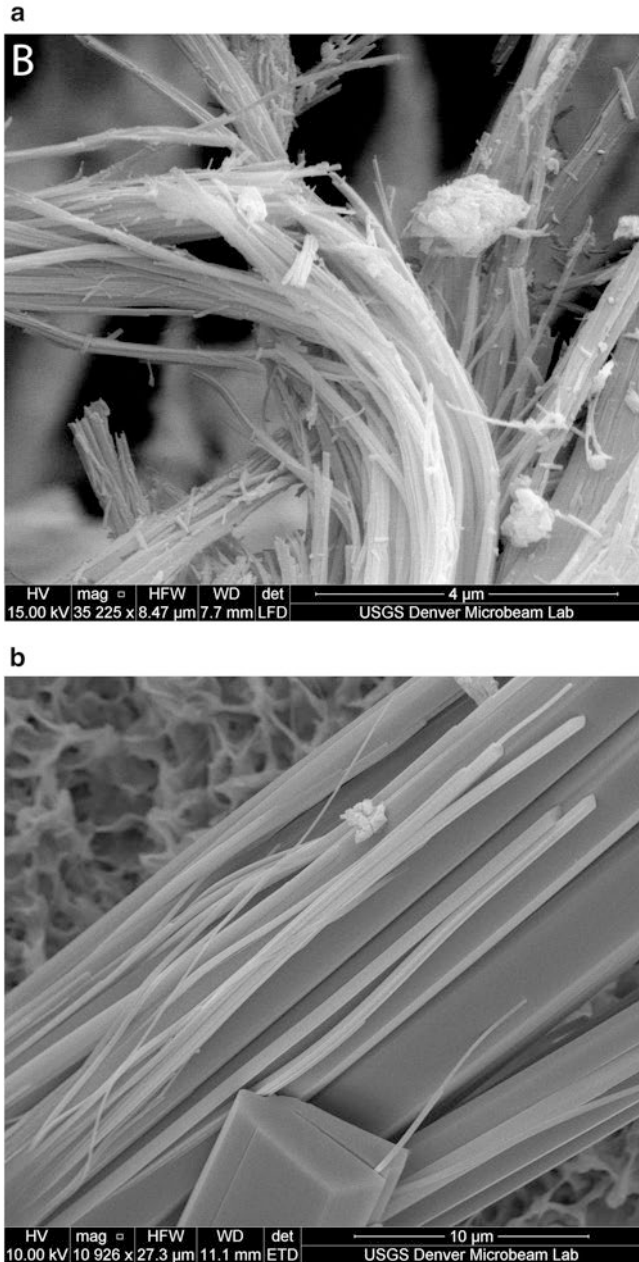


Fig. 2.12 Erionite. (a) Woolly erionite from Rome, Oregon, displaying an asbestiform habit. (b) Fibrous erionite from Pima County, Arizona. Most fibers are a few micrometers or more in width, although very fine, asbestiform fibers are also present. The two habits likely represent two periods of fiber formation. SEM micrographs courtesy of Van Gosen et al. (2013)

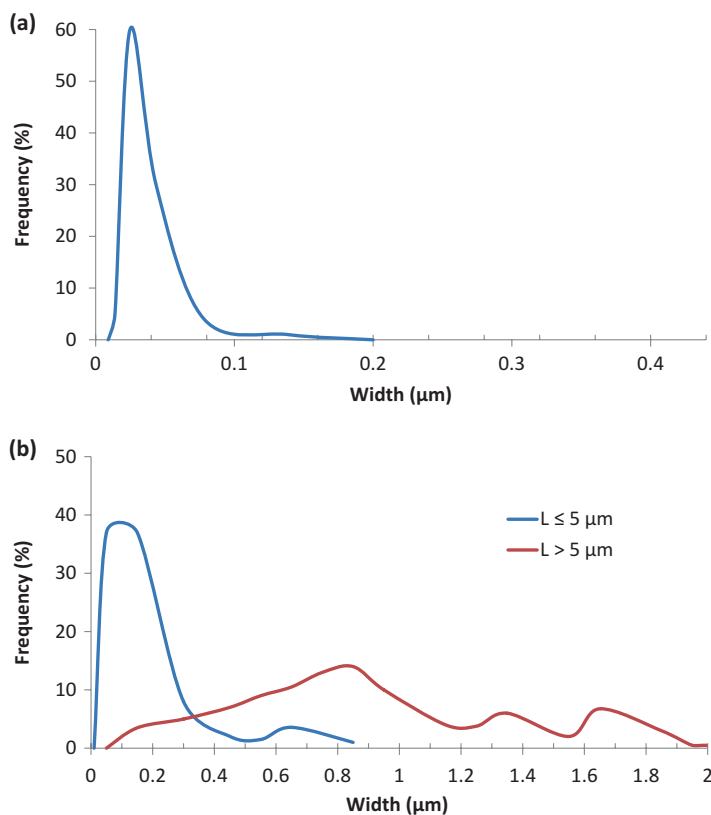


Fig. 2.13 Frequency of width of two erionite samples from Shedd et al. (1982). (a) Woolly erionite from Lander County, Nevada. The longest fiber included in the distribution is 9.7 μm and 6% are ≥ 5 μm in length. In this asbestiform erionite, width increases only slightly with length. (b) Fibrous, nonasbestiform erionite from Pershing County, Nevada. The longest common erionite particle measured is 20.6 μm; width increases systematically with length

Not all erionite is asbestiform. It may be found in prismatic or acicular particles and in more massive amygdaloidal form. Erionite in different habits may be found at the same location as shown in Fig. 2.12b. Elongated particles of nonasbestiform erionite may resemble those of common amphibole.

Figure 2.13a illustrates the frequency distribution of the width of woolly erionite fibers from Nevada (after Shedd et al. 1982). The variance in width is very small, with most fibers between 0.03 and 0.05 μm. The modal width of woolly erionite from Durkee, Oregon, is reported to be 0.016 μm (Matassa et al. 2015). The disaggregated fibrils from both locations are commonly less than 5 μm in length, although fibers and fiber bundles of 50 μm or more may occur. Gude and Sheppard (1981) reported fibers up to 10 mm in length. Other minerals intergrown with erionite fibers may inhibit disaggregation into the component fibrils. In Fig. 2.13b, the width frequency distribution typical of common erionite from Nevada is depicted. The modal width of short common erionite EMPS is 0.1–0.2 μm; longer particles have widths that range widely.

2.8 The Identification of Asbestos and Woolly Erionite, and the Characterization of Particle Populations

Mineral occurrences that have the potential to form long thin respirable fibers can be recognized in hand samples by their silky luster and their ability to readily separate into visible fibers by hand pressure. Under the optical microscope, asbestos is recognized by the following characteristics (EPA 1993), which also hold for woolly erionite:

1. Mean aspect ratios (length/width) ranging from 20:1 to 100:1 or higher for fibers longer than 5 μm (aspect ratio determined for individual fibers, not bundles)
2. Very thin fibrils, usually less than 0.5 μm in width, and
3. Two or more of the following:
 - a. Parallel fibers occurring in bundles
 - b. Fiber bundles displaying splayed ends
 - c. Matted masses of individual fibers
 - d. Fibers showing curvature

Under the electron microscope, the designation of a single EMP that is not composed of multiple fibrils as a fiber or a fragment can be very difficult. This is particularly true if the particle is short. Wylie et al. (1985) have shown that for amphibole EMPs of a few micrometers or less, the widths of fibers and fragments converge, and dimensions become unreliable discriminators. For longer particles, there are sufficient dimension data on populations of amphibole-asbestos and amphibole cleavage fragments to provide general discriminating criteria, but applying them to a single particle is difficult. Van Orden et al. (2008) describe characteristics of fibers and fragments that may be helpful for narrow EMPs ($\approx 0.5 \mu\text{m}$ or less) that are not fiber bundles. A summary is provided in Table 2.2.

While it is accepted that dimensions of mineral particles are important factors in determining carcinogenicity, representation of those dimensions in ways that are meaningful for a quantitative assessment of risk is challenging. These challenges arise for many reasons, but important among them are: (1) the distributions of length and width are not normal, (2) short fibers are much more abundant than long fibers, but it is the long fibers that are of the most interest biologically, (3) fibers disaggregate into their component fibrils differently depending on their history and degree of manipulation, (4) the range of length may be several orders of magnitude greater than the range in width, and (5) with only a few exceptions, longer fibers contain a higher proportion of the mass of the population than shorter fibers. During preparation of bulk samples for characterization, grinding of the material has been used. For the higher tensile strength fibers, such as crocidolite, amosite, chrysotile and woolly erionite, hand grinding has limited impact on length distributions, but for the more brittle materials, fiber lengths can be significantly reduced by even a small amount of grinding. Grinding rarely breaks asbestos fibrils longitudinally, but may contribute to their disaggregation. The instrumentation used to characterize a mineral par-

Table 2.2 Representative magnitudes of the frequency of width of amphibole fibers and fragments with length $>5 \mu\text{m}$ (Wylie 2016)

Mineral name and location	$\% \leq 0.25 \mu\text{m}$	$\% \leq 0.33 \mu\text{m}$	$\% \leq 0.5 \mu\text{m}$
<i>1. Airborne and lung burden</i>			
Crocidolite, cape asbestos province, South Africa	75	90	99
Amosite, Transvaal asbestos range, South Africa	20	45	70
Na-Ca amphibole-asbestos, Libby and Italy	20	45	70
Anthophyllite-asbestos, Finland	5	15	45
Brittle amphibole mining aerosol	Trace	2	7
<i>2. Laboratory-prepared samples</i>			
Tremolite-asbestos, Korea	50	70	80
Preskaite, Transvaal asbestos range, South Africa	20	45	70
Tremolite-asbestos, Udaipur, India	7	15	30
Brittle amphibole	Trace	2	6

ticle population is also an important factor. The very narrow width of asbestos and woolly erionite fibrils limits the use of optical microscopy. The full range of length may be impossible to characterize by TEM, while the smallest fibril widths may be difficult to measure by SEM. Ultrasound disaggregates fibers into their component fibrils, but the degree to which this happens varies among samples and with time of sonication. Sampling protocols may or may not designate a minimum aspect ratio or length. Accessory minerals, sometime fibrous, may or may not be included. Samples are sometimes dispersed in water and selectively sampled by settling times or column depth. In comparing population characterizations, it is important that protocols be considered.

Length distributions can be modeled by the relationship $\log N = -D \log L + C$, where N is the number of fibers with a length greater than L , C is a constant, and D is the fractal dimension (Wylie, 1993). Turcotte (1986) concluded that the fractal dimension is a measure of the resistance of the material to fragmentation. While this is true of fragmented material, in the case of high tensile strength asbestos fibrils that do not fragment, D reflects the ease of disaggregation into component fibrils over the range of length measured.

The relationship between log length and log width in particle populations can be expressed by the relationship: $\log \text{width} = F \log \text{length} + b$, where F is the fibrosity index (Siegrist and Wylie 1980). Small values of F are characteristic of greater fibrosity, as they are derived from populations in which the aspect ratios are high and widths are nearly constant; larger values of F imply more brittle behavior, with lower aspect ratios and variable widths that increase with length. For asbestos and woolly erionite, the fibrosity index is normally less than 0.2; for populations that contain both byssolite and asbestos, F as large as 3.4 has been reported.

The fibrosity indices characteristic of fragments of common amphibole and common erionite are greater than 0.7 (Siegrist and Wylie 1980, Shedd 1985).

The arithmetic means of width and length are not recommended as population parameters for describing asbestiform fiber. The geometric mean may be somewhat useful for width, but it has limitations for length, especially for characterization of bulk samples. Modal width for specific length segments may be the most useful descriptive statistic for comparing populations. This approach has been used in Table 2.2, which provides data on selective amphibole EMPs from a variety of sources.

2.9 Summary

Amphibole and erionite are biodurable. Their surface area (per unit weight) is largely controlled by width. Among asbestiform minerals, woolly erionite is composed of the narrowest fibrils, followed by commercially produced chrysotile, crocidolite, amosite and anthophyllite-asbestos, in that order. Asbestiform amphibole in the tremolite-actinolite-ferroactinolite, edenite, richterite, and winchite series occur with fibrils that range in size from crocidolite to anthophyllite-asbestos to byssolite; many occurrences are characterized inhomogeneous fibrils sizes.

Width frequency data from Wylie (in press) for EMPs >5 μm in length are summarized in Table 2.2. While widths for asbestos range widely, narrow widths are uncommon among cleavage fragment populations. Width ultimately controls the penetration of an EMP into the lung while length may be the major factor (other than biodurability) in controlling its residence time. Both dimensions are important in understanding mesotheliomagenicity of minerals.

References

- Addison J, Davies LST (1990) Analysis of amphibole asbestos in chrysotile and other minerals. *Ann Occup Hyg* 34:159–175
- Atkinson GR, Rose D, Thomas K, et al. (1981) Collection, analysis and characterization of vermiculite samples for fiber content and asbestos contamination. Midwest Research Institute report for the US Environmental Protection Agency Project 4901-A32 under EPA Contract 68-01-5915, Washington, DC
- Beard ME, Ennis JT, Crankshaw OS, et al. (2007) Preparation of nonasbestiform amphibole minerals for method evaluation and Health Studies Summary Report and appendices. Prepared for Martin, Harper, NIOSH, Morgantown, WV by RTI International. (Hearl F, Personal communication, CDC/NIOSH/OD)
- Bish DL, Chipera SJ (1991) Detection of trace amounts of erionite using X-ray powder diffraction: erionite in tuffs of Yucca Mountain, Nevada, and central Turkey. *Clay Clay Miner* 39:437–445
- Bish DL, Ming DW (eds) (2001) Natural zeolites: occurrence, properties, applications, Reviews in mineralogy and geochemistry, vol 45. Mineralogical Society of America, Washington, DC

- Bloss FD (1971) Crystallography and crystal chemistry: an introduction. Holt, Rinehart and Winston, New York, NY
- Cametti G, Pacella A, Mura F et al (2013) New morphological chemical and structural data of woolly erionite-Na from Durkee, Oregon, USA. *Am Mineral* 98:2155–2163
- Campbell WJ, Huggins CW, Wylie AG (1980) Chemical and physical characterization of amosite, chrysotile, crocidolite, and nonfibrous tremolite for oral ingestion studies by the National Institute of Environmental Health Sciences. US Bureau of Mines Report of Investigations 8452. United States Department of the Interior.
- Deer WA, Howie RA, Zussman J (1997) Rock forming minerals. Volume 2B: double-chain silicates, 2nd edn. The Geological Society, London
- Deer WA, Howie RA, Wise WS et al (2004) Rock forming minerals. Volume. 4B: framework silicates; silica minerals, feldspathoids and the Zeolites, 2nd edn. The Geological Society, London
- Deer WA, Howie RA, Zussman J (2009) Rock forming minerals. Volume 3B: layered silicates; excluding micas and clay minerals. The Geological Society, London
- Dogan AU, Dogan M (2008) Re-evaluation and reclassification of erionite. *Environ Geochem Health* 30:355–366
- Dorling M, Zussman J (1987) Characteristics of asbestiform and nonasbestiform calcic amphiboles. *Lithos* 20:469–489
- Eborn SK, Aust AE (1995) Effect of iron acquisition on induction of DNA single-strand breaks by erionite, a carcinogenic mineral fiber. *Arch Biochem Biophys* 316:507–154
- Ecology and Environment, Inc (EEI) (2005) El Dorado Hills naturally occurring asbestos multimedia exposure assessment. El Dorado Hills, California Preliminary Assessment and Site Inspection Report Interim Final, LabCor Contract No. 68-W-01-012; TDD No.: 09-04-01-0011; Job No.: 001275.0440.01CP (Lee RJ, personal communication)
- EPA (1993) Test Method: method for the determination of asbestos in bulk building materials. Perkins RL, Harvey BW. EPA/600/R-93/116
- EPA US (2006) U.S. Environmental Protection Agency Produced Access Database, Libby Montana airborne particles; in the matter of United States of America vs. WR Grace, et al, CR-05-070 M-DWM (*D. Montana*), 2005–2006 (Lee RJ, personal communication)
- Gianfagna A, Andreozzi B, Ballirano P et al (2007) Structural and chemical contrasts between prismatic and fibrous fluoro-edenite from Biancavilla, Sicily, Italy. *Can Mineral* 45:249–262
- Gibb GW, Hwang CY (1980) Dimensions of airborne asbestos fibers. In: Wagner JC (ed) Biological effects of mineral fibers, vol 1. IARC Scientific Publication #30, Lyon, pp 69–77
- Greenwood WS (1998) A mineralogical analysis of fibrous talc. Master of Science Thesis, Department of Geology, University of Maryland, College Park, MD
- Gude AJ, Sheppard RA (1981) Woolly erionite from the Reese River zeolite deposit, Lander County Nevada and its relations to other erionites. *Clay Clay Miner* 29:378–384
- Guthrie G, Mossman B (eds) (1993) Health effects of mineral dusts, Reviews in mineralogy, vol 28. Mineralogical Society of America, Washington
- Harper M, Lee EG, Doorn SS et al (2008) Differentiating non-asbestiform amphibole and amphibole asbestos by size characteristics. *J Occup Environ Hyg* 5:761–770
- Hawthorne FC, Oberti R, Ventura GD, Mottana A eds (2007) Amphiboles: Crystal Chemistry, Occurrence, and Health Issues. Reviews in Mineralogy. Vol. 67. Mineralogical Society of America, Washington DC
- Hawthorne FC, Oberti R, Harlow GE, Maresch WV, Martin RF, Schumacher SC, Welch MD (2012) Nomenclature of the amphibole supergroup. *Am Miner* 97:2031–2048.
- Hodgson AA (1979) Chemistry and physics of asbestos. In: Michaels L, Chissick SS (eds) Asbestos. Vol. 1. Applications and Hazards. Wiley, New York, pp 67–114
- Hume LA, Rimstidt JD (1992) The biodegradability of chrysotile asbestos. *Am Mineral* 77: 1125–1128
- Keeling JL, Raven MD, Self PG, et al. (2008) Asbestiform antigorite occurrence in South Australia. Proc 9th Int Conf Applied Mineralogy, Brisbane, Australia, pp 329–336

- Leake BE, Woolley AR, Arps CES et al (1997) Nomenclature of amphiboles: report of the Subcommittee on Amphiboles of the International Mineralogical Association, Commission on New Minerals and Mineral Names. *Can Mineral* 35:219–246
- Leake BE, Woolley AR, Birch WD et al (2004) Nomenclature of amphiboles: additions and revisions to the International Mineralogical Association's amphibole nomenclature. *Am Mineral* 89:883–887
- Lippmann M, Timbrell V (1990) Particle loading in the human lung: human experience and implications for exposure limits. *J Aerosol Med* 3:S155–S168
- Matassa R, Familiari G, Relucenti M et al (2015) A deep look into erionite fibres: an electron microscopy investigation of their self-assembly. *Sci Report* 5:16757
- Meeker GP, Bern AM, Brownfield IK et al (2003) The composition and morphology of amphiboles from the Rainy Creek Complex, near Libby Montana. *Am Mineral* 88:1955–1969
- Mumpton FA, Thompson CS (1975) Mineralogy and origin of the Coalinga asbestos Deposit. *Clay Clay Miner* 23:131–143
- NIOSH (2011) Asbestos fibers and other elongate mineral particles: state of the science and road-map for research. *Current Intelligence Bulletin* 62. DHHS:CDC Pub. No. 2011–159
- Nolan RP, Langer AM, Ross M et al (eds) (2001) Health effects of chrysotile asbestos: contribution of science to risk-management decisions. Mineralogical Society of Canada, Ontario. Special publication 5
- O'Hanley DS (1986) The origin and mechanical properties of asbestos. Master of Science thesis, University of Minnesota, Twin Cities, MN
- Paoletti L, Bruni BM (2009) Caratterizzazione dimensionale di fibre anfiboliche nel polmone e nella pleura di cassi di mesothelioma da esposizione ambientale. *Med Lav* 100:11–20
- Pooley FD, Clark N (1980) A comparison of fibre dimensions in chrysotile, crocidolite and amosite particles from sampling of airborne dust and from post mortem lung tissue. *IARC Sci Publ* 30:79–86
- Redwood SD (1993) Crocidolite and magnesite associated with lake superior-type banded iron formation in Chapare Group of eastern Andes, Bolivia. *Institution of Mining and Metallurgy. Section B: Appl Earth Sci* 102:114–122
- Shedd KB (1985) Fiber dimensions of crocidolites from Western Australia, Bolivia, and the Cape and Transvaal Provinces of South Africa. *US Bureau of Mines Report of Investigations* 8998. US Department of the Interior
- Shedd KB, Virta RL, Wylie AG (1982) Size and shape characterization of fibrous zeolites by electron microscopy. *Bureau of Mines Report of Investigations* 8674. US Department of the Interior
- Siegrist HG, Wylie AG (1980) Characterizing and discriminating the shape of asbestos particles. *Environ Res* 23:348–361
- Timbrell V (1975) Alignment of respirable asbestos fibres by magnetic fields. *Ann Occup Hyg* 18:299–311
- Timbrell V, Pooley F, Wagner JC (1970) Characteristics of respirable asbestos fibers. *Proc Int Conf Pneumoconiosis*, Shapiro HA (ed), Oxford University Press, pp 120–125
- Turcotte DL (1986) Fractals and Fragmentation. *J Geophys Res* 91:1921–1926
- Van Gosen B (2007) The geology of asbestos in the United States and its practical applications. *Environ Eng Geosci* 13:55–68
- Van Gosen BS, Blitz TA, Plumlee GS et al (2013) Geologic occurrences of erionite in the United States: an emerging national public health concern for respiratory disease. *Environ Geochem Health* 35:419–413
- Van Orden DR, Allison KA, Lee RJ (2008) Differentiating amphibole asbestos from non-asbestos in a complex mineral environment. *Indoor Built Environ* 17:58–68
- Verkouteren JR, Wylie AG (2002) Anomalous optical properties of fibrous tremolite, actinolite and ferro-actinolite. *Am Mineral* 87:1090–1095
- Watson MB (1999) The effect of intergrowths on the properties of fibrous anthophyllite. Master of Science thesis, Department of Geology, University of Maryland, College Park, MD
- Wylie AG (1979) Optical properties of the fibrous amphiboles. *Ann N Y Acad Sci* 330:600–605

- Wylie AG (1993) Modeling asbestos populations: a fractal approach. *Can Mineral* 30:437–446
- Wylie AG (2016). Amphibole dust: asbestos fibers, fragments, and mesothelioma. *Canadian Mineral* (in revision)
- Wylie AG, Candela PA (2015) Methodologies for determining the sources, characteristics, distribution and abundance of asbestiform and nonasbestiform amphibole and serpentine in ambient air and water. *J Toxicol Environ Health Part B: Crit Rev* 18:1–42
- Wylie, AG, Virta, RL (2016) Size distribution measurements of amosite, crocidolite, chrysotile, and nonfibrous tremolite: digital Repository at the University of Maryland, College Park, MD. <http://dx.doi.org/10.13016/M2798Z>
- Wylie AG, Shedd KB, Taylor ME (1982) Measurement of the thickness of amphibole asbestos fibers with the scanning electron microscope and transmission electron microscope. In: Heinrich KFJ (ed) *Microbeam Analysis*. San Francisco Press, San Francisco, CA, pp 181–187
- Wylie AG, Virta R, Russek E (1985) Characterizing and discriminating airborne amphibole cleavage fragments and amosite fibers: implications for the NIOSH Method. *Am Ind Hyg Assoc J* 46:197–201
- Wylie AG, Virta RL, Shedd KB, et al. (2015) Size and shape characteristics of airborne amphibole asbestos and amphibole cleavage fragments. Digital Repository at the University of Maryland, <http://dx.doi.org/10.13016/M2HP87>



<http://www.springer.com/978-3-319-53558-6>

Asbestos and Mesothelioma

Testa, J.R. (Ed.)

2017, VIII, 407 p. 65 illus., 43 illus. in color., Hardcover

ISBN: 978-3-319-53558-6